ANALYSIS OF THE GENERATION OF GUIDED WAVES USING FINITE SOURCES: AN EXPERIMENTAL APPROACH

Krishna M. Rajana, Derrick Hongerholt, Joseph L. Rose
Department of Engineering Science & Mechanics
Pennsylvania State University
University Park, PA 16801

John J. Ditri
Strainoptic Technologies, Inc.
108 W. Montgomery Ave.
North Wales, PA 19454

INTRODUCTION

The wedge method of generating guided waves in isotropic layers, originally analyzed theoretically and experimentally by Viktorov and colleagues [1-2], has recently been extended to encompass generally anisotropic layers and transducers with arbitrary pressure distributions [3-4]. One result of these analyses was that there is a continuous dependence of the excitation amplitude of any given mode on the incident angle of the wedge. In [3-4], explicit expressions were given for the excitation amplitude as a function of incident angle; given the transducer size, pressure profile and frequency. In this paper, predictions in [3-4] are tested against laboratory experiments to asses their validity.

BACKGROUND AND THEORETICAL CONSIDERATIONS

In the wedge method of generating guided waves, a piezoelectric transducer is mounted to a wedge which is inclined at an angle θ_i to the surface of the layer. The wedge itself is coupled to the layer via a thin film of non-viscous liquid. Alternatively, the transducer and specimen can be immersed in a fluid which then assumes the role of the wedge. All experimental results to follow have in fact been obtained by an immersion method.

An analysis of a two-dimensional model of the wedge method, applicable to arbitrary pressure distributions and generally anisotropic layers, has been carried out

Review of Progress in Quantitative Nondestructive Evaluation, Vol. 14
Edited by D.O. Thompson and D.E. Chimenti, Plenum Press, New York, 1995

Table I. Modes used in the experimental study and some of their acoustical properties.

Mode	fd [MHz·mm]	V_{phase} [mm/μsec]	Wavelength [mm]
S_0	0.914	5.38	5.8
S_0	1.013	5.30	2.4
S_1	4.572	5.78	2.6
S_2	7.143	6.47	2.9

recently [4]. In that work, the transducers were assumed to be infinite in one dimension, thus creating a state of plane strain deformation in the layer. For simplicity, the time variation of the loading was assumed to be harmonic, i.e., $e^{i\omega t}$. Denoting by $A_\nu(z;\omega,\theta_i)$ the "z" dependent amplitude with which mode "ν" of the layer is excited by the transducer with frequency ω and incident angle θ_i, it was shown that for a layer of thickness b,

$$A_\nu(z;\omega,\theta_i) = \frac{\tilde{v}_{\nu y}(b/2)}{4P_{\nu\nu}} \frac{e^{-ik_\nu z}}{\cos(\theta_i)} \int_{-\infty}^{\infty} p(\alpha) e^{i\chi\alpha}\, d\alpha \tag{1}$$

where,

$$\chi \triangleq \frac{k_\nu - k_w \sin\theta_i}{\cos\theta_i}. \tag{2}$$

In Eq. (1), $\tilde{v}_{\nu y}(b/2)$ denotes the complex conjugate of the "y" component of the particle velocity of mode "ν" underneath the wedge and $P_{\nu\nu}$ denotes the time average power flux carried along the layer by the mode ν per unit waveguide width [5].

The term $p(\alpha)$ in Eq. (1) denotes the pressure profile across the face of the transducer. In [3] and [4], simple forms were assumed for $p(\alpha)$ which allowed expressions to be obtained for $A_\nu(z;\omega,\theta_i)$ analytically. This permitted a detailed investigation into the affect the size of the transducer D, the incident angle and the pressure distribution had on the excitation amplitude of any given mode. In this work, direct measurement of $p(\alpha)$ was performed for several transducers of varying frequencies and nominal sizes. Using the measured profiles, Eq. (1) was numerically integrated to obtain theoretical predictions for the variation of the excitation amplitude of a given mode as a function of the incident angle of the transducer. The actual variation of excitation amplitude of several modes was directly measured (using an experimental arrangement described later) and compared to the theoretical predictions. Although beam spreading was neglected in the theoretical analysis, it was partially accounted for in the experiments because the "actual" transducer sizes (D_a) were taken as the -14 dB points in the experimentally obtained $p(\alpha)$ curves. Due to beam spreading, this width exceeded the physical size of the transducer.

The modes/points chosen for study are listed in Table I. The choice of these points is based upon consideration of the excitability of the modes and in an attempt to maximize the group velocity. The chosen points cover a moderate range

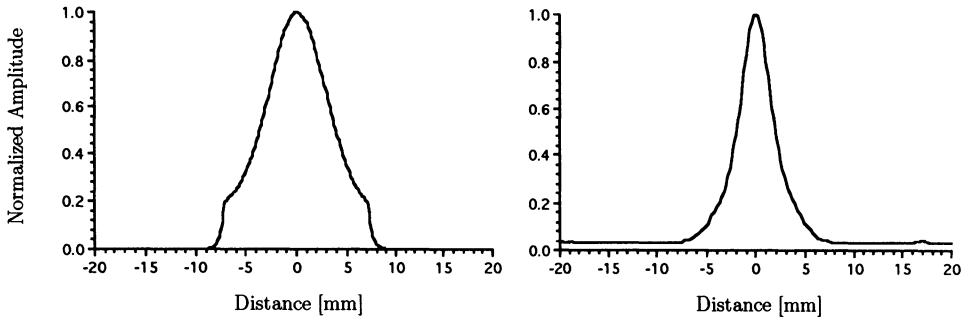

Fig. 1. Two typical normalized pressure profiles. Transducer on left was driven at 0.9 MHz and had a nominal diameter of 12.7 mm. Transducer on right was driven at 2.25 MHz and had a nominal diameter of 6.35 mm.

of frequencies and wavelengths. To isolate an individual mode for the purposes of theoretically generating the excitation amplitude versus incident angle curve, that mode's wavenumber k_ν, particle velocity field at the surface of the layer $\tilde{v}_{\nu y}(b/2)$ and the power flux $P_{\nu\nu}$ must be calculated for a frequency equal to the center frequency of the transducer used. This information was then used along with the experimentally measured pressure profile of the transducer in Eq. (1).

DESCRIPTION OF DATA ACQUISITION SYSTEM

Standard, commercially available transducers of two different nominal frequencies (1.0 and 2.25 MHz) were used in this study. Three 1.0 MHz transducers and two 2.25 MHz transducers of different diameters were used. All transducers had circular piezoelectric elements with nominal diameters ranging from 6.35 to 19.05 mm. The transducers were driven by approximately ten cycles of a (rectangular) gated sinusoidal tone burst with a center frequency of 0.9 MHz for the 1.0 nominal transducers and 2.25 MHz for the nominal 2.25 MHz transducers. The chosen number of cycles was sufficient to ensure a frequency bandwidth of less than 15% at the -6 dB level. The use of a rectangular gate caused the presence of side lobes in the frequency spectrum which were, in all cases, at around a -15% dB level compared to the principal maximum. High precision computer controlled linear translation and rotation stages were used to perform the experiments. The data acquisition system included a 100 MHz Sonix STR8100 digitizer and an NCR 386 personal computer.

TRANSDUCER CHARACTERIZATION

The five transducers used in this study were first characterized by experimentally measuring the pressure profiles across their diameter. In an immersion tank, the transducer was used as a sender and a roughly 1 mm diameter pin-ducer, located at twice the near field of the sender, was used as a receiver. After locating the maximum in the pressure profile (at the center of the transducer) the transducer was traversed over a 20 mm distance with a 0.2 mm increment on either side of the maximum, giving a total of 400 points and 40 mm scan length. The data was smoothed by replacing each measured point with the average of it with its nearest two neighbors; a process which was done twice. The profiles were then normalized

Table II. Nominal and "Actual" diameters of the five transducers tested.

Frequency [MHz]	Nominal Diameter [mm]	Actual Diameter (D_a) [mm]
0.90	19.05	27.69
0.90	12.70	21.00
0.90	9.52	18.65
2.25	12.70	15.68
2.25	6.35	9.72

to unity maximum by dividing by the maximum value. The data points on the left and right of the maximum with amplitudes below 0.2 (i.e., -14dB) were forced to decay exponentially with distance from the center. This was done to remove the electrical noise which was present at this low amplitude level. The width of the profile at the 0.2 (-14dB) level was called the "actual" size of the transducer, D_a. They are listed, along with the nominal (physical) size in Table II for the five transducers tested. Shown in Fig. 1 are two typical profiles obtained in this manner.

A cubic spline interpolant was obtained for each measured profile. This served as $p(\alpha)$ in the integrand of Eq. (1) which was, after selecting a given mode, numerically integrated. Sample theoretically predicted excitation amplitudes are shown, along with the corresponding experimentally obtained curves, in the next section.

DIRECT MEASUREMENT OF EXCITATION AMPLITUDES

In order to experimentally measure the excitation amplitude of a given mode for a given transducer, an immersion setup was employed. A plate of a given thickness (b) was mounted onto a computer controlled rotatable turntable which was immersed in a water tank. The transducer was also immersed and aligned relative to the plate so that the center of the emitted beam struck as nearly as possible the axis of rotation of the plate (Fig. 2). This excited Lamb waves in the plate which propagated along the plate until reaching the end, where they were reflected and returned to the sender. The amplitude of the returning Lamb wave was detected by the transducer due to leakage into the surrounding water. The distance from the axis of rotation to the end of the plate was two inches (50.8 mm) in all cases. The distance from the transducer to the axis of rotation was twice the near field of the sender ($2N$), calculated based on the driving frequency and nominal diameter of the transducer.

The maximum amplitude in a gated portion of the received signal was recorded as the plate was rotated over a range of angles which depended upon the mode chosen. The angular increment in each case was 0.2 degrees. Care was required in gating the received signal to isolate a given mode since in many cases modes with nearly coincident phase velocities were excited. Time gates to isolate given modes were chosen according to theoretically calculated group velocities and known propagation lengths. This was not a problem in most cases, since differing group velocities caused separation of the modes but proved to be a problem when the group velocities of the generated modes was also similar.

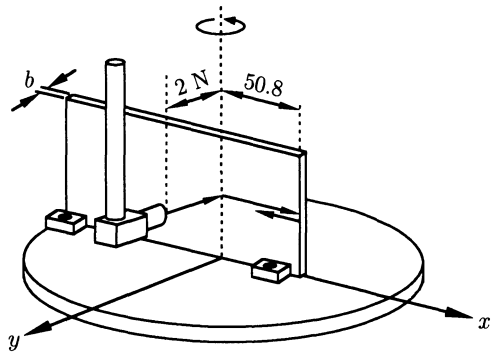

Fig. 2. Experimental setup for experimentally measuring the excitation amplitude of a given mode as a function of incident angle of the source.

In order to excite different modes, as well as the same mode with different wavelengths, while using only two different frequencies, aluminum plates of four different thicknesses were used. For the 0.9 MHz transducers, a 1.016 mm thick plate was used to isolate the S_0 mode at a frequency thickness product (fd) of 0.9144 MHz·mm. The 2.25 MHz transducers were used on plates of 0.432, 2.032 and 3.175 mm to generate modes S_0, S_1 and S_2 at fd's of 1.01, 4.57 and 7.14 MHz·mm respectively. The experimentally obtained excitation amplitude versus incident angle curves were normalized to unity maximum in order to compare them to the theoretically generated curves.

RESULTS AND DISCUSSION

Results for the excitation of the S_0 mode in a 1.016 mm aluminum plate using three different size transducers, all driven at 0.9 MHz are presented in figure 3. The dashed lines represent experimentally obtained profiles and the solid lines represent theoretical curves. Because of uncertainty in absolute measurement of incident angle, the theoretical curves were shifted when necessary (in no case by more than 1 degree) to make the principal maxima coincide. Several observations can be made concerning these results. First, there is good overall agreement between theory and experiment for the 27.69 and 21.00 mm transducers, whereas the experimental curve for the 18.65 mm transducer is considerably wider than the theoretically predicted curve. Each set of experiments was performed twice to asses repeatability, which was excellent in all cases. Notice that as the (actual) size of the transducer decreases, the widths of both the theoretical and experimental profiles increase. It may be noted that in this set of experiments, the only variable is source size; the other critical parameters such as Snell's law angle (based on the S_0 mode phase velocity at the given fd product), excitation frequency (hence the wavelength in the plate, λ^0) and the wavelength in coupling medium being held constant.

The -1.80% and 12.6% difference between the -6 dB widths of the theoretical and experimental profiles for the sources of 27.69 and 21.00 mm respectively, are considered acceptable, especially considering differences between theoretical assumptions and the actual experimental setup. The difference associated with the source of 18.65 mm is 53.0% and this is considered too large to attribute to experimental error. It is believed that beam spreading affects which have been neglected

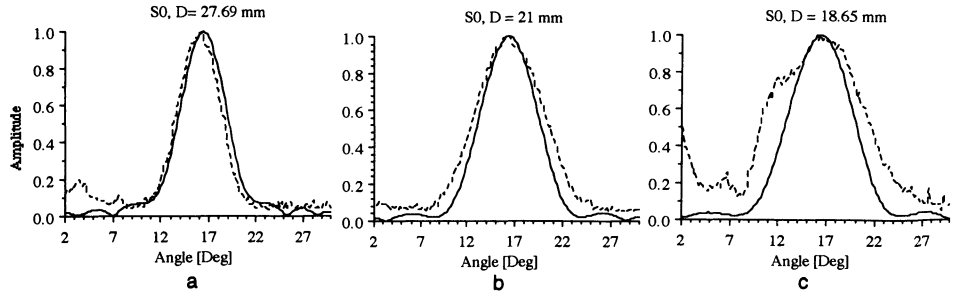

Fig. 3. Experimental results for the generation of S_0 mode at a frequency thickness product of 0.9144 MHz·mm with transducers of varying actual diameters, D_a. Solid lines: Theory, Dashed lines: Experiment. (a) $D_a = 27.69$ mm, (b) $D_a = 21.00$, (c) $D_a = 18.65$ mm

in the theory but are of course present in the experiment contribute to the deviation. Beam spreading effects become more important when either the nominal size of the transducer or its driving frequency decrease. Based on the nominal diameters of the transducers used in cases (a), (b) and (c), along with the driving frequency of 0.9 MHz, and a speed in water of 1.5 mm/μsec, the half angles of beam divergence calculated using the standard formula $\sin(\alpha) = 0.6v_{\text{water}}/fD$ are $\alpha = 3.0$, 4.5 and 6.0 degrees respectively.

In a second set of experiments, the S_0 mode was generated at an fd product of 1.0125 MHz·mm using a 2.25 MHz transducer and an aluminum plate of 0.432 mm thickness. This is nearly the same point as generated in the previous experiments (with $fd = 0.9144$) but the frequency was more than doubled and the plate thickness was correspondingly less than half, so that fd was kept roughly the same. A transducer with a $D_a = 15.68$ mm was used. The collected profile is shown in Fig. 4a along with a repetition of Fig. 3b. This comparison shows that it is not only the size of the transducer which determines the width of the angular spectrum but its frequency as well. The higher the frequency, the narrower the width of the amplitude excitation profile. Notice that this effect is captured remarkably well in the theoretical prediction with a difference between the -6dB widths from theory and experiment of less than 5%. The half angle of beam divergence for the 2.25 MHz transducer with a nominal diameter of 15.68 mm is $\alpha = 1.8$ degrees. Note also that although the actual diameters of the transducers used to generate Fig. 4a and 4b are around 25% different, this difference in size would cause the opposite effect as that which has occurred (i.e., it would tend to make the two widths closer), showing that the dominant cause of the difference in width is due to the difference in frequency.

As a final set of experiments, 2.25 MHz transducers with actual diameters $D_a =$ 15.68 and 9.72 mm were used to generate modes S_1 and S_2 at frequency thickness products of 4.572 and 7.143 MHz·mm respectively. The experimental and theoretical amplitude profiles are shown in Fig. 5 along with a repetition of the S_0 profiles for completeness. Note that there are two peaks present in the experimental curves

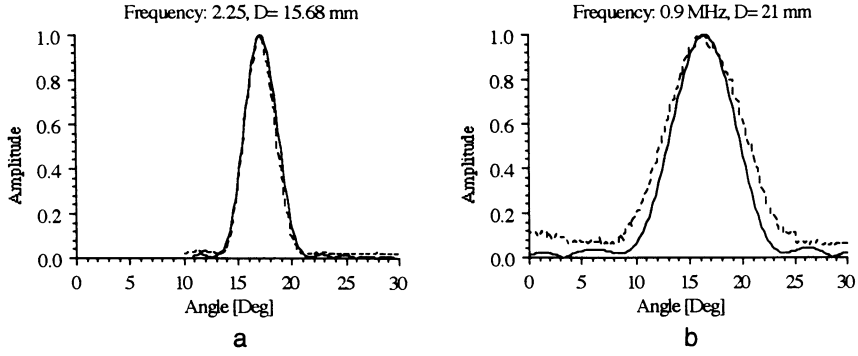

Fig. 4. Experimental results for the generation of the S_0 mode at roughly the same fd but with different f's and d's. Solid lines: Theory, Dashed lines: Experiment. (a) fd = 1.0125 MHz·mm, D_a = 15.68 mm, (b) fd = 0.9144 MHz·mm, D_a = 21.0 mm.

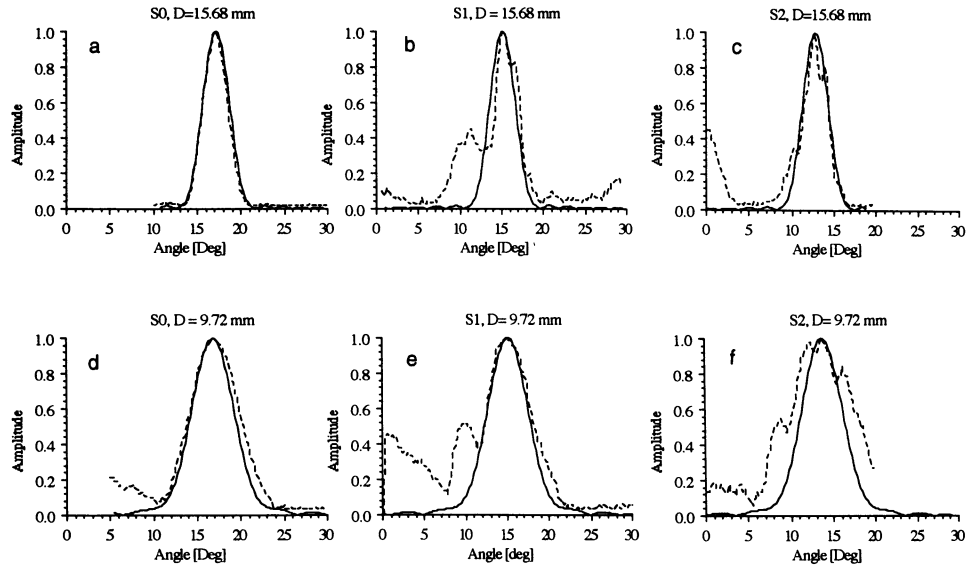

Fig. 5. Experimental results for the generation of modes S_0, S_1 and S_2 at fd's of 0.91, 4.57 and 7.14 MHz·mm respectively. Solid lines: Theory, Dashed lines: Experiment. (a) S_0, D_a = 15.68 mm, (b) S_1, D_a = 15.68 mm, (c) S_2, D_a = 15.68 mm, (d) S_0, D_a = 9.72 mm, (e) S_1, D_a = 9.72 mm, (f) S_2, D_a = 9.72.

of Fig. 5b and 5c. This is due to the simultaneous excitation of S_1 and S_2. The theory curve has been generated assuming excitation of only S_1 and therefore has only one peak. Similar observations can be made concerning these profiles as has been made concerning the others. The width of the amplitude profile of any given mode increases as the actual size of the transducer decreases. The agreement between theory and experiment generally degrades as either the nominal size or the driving frequency of the transducer decreases. Both of these effects cause larger beam spreading which has been completely neglected in the theory.

CONCLUSIONS

Based on the comparisons of theory to experiment for all of the cases presented, it is concluded that the theory developed in [3] and [4] gives satisfactory results for predicting the width of the excitation spectrum of a given Lamb wave mode using a particular transducer. The discrepancy between theoretically predicted and experimentally obtained results increases as the beam spread of the source transducer increases. Beam spreading causes both a widening of the beam waist *and* a system of non-parallel rays in the incident beam. While the widening of the beam waist was accounted for by using the actual beam profiles and numerical integrations, the non-parallel rays in the beam bundle were completely unaccounted for in the theory. Also not accounted for in the theory is the circular nature of the transducers used; in the theory, strip sources (2 dimensional) were assumed.

ACKNOWLEDGMENTS

This work was supported by Dr. Alex Vary of the NASA Lewis Research Center, Cincinnati, OH., and Mr. Dave Gallela of the Federal Aviation Agency Technical Center, Atlantic City, NJ.

REFERENCES

1. VIKTOROV, I.A., ZUBOVA, O.M., and KAEKINA, T.M., "Investigation of Lamb Wave Excitation by the "Wedge" Method," *Soviet Physics-Acoustics*, Vol. 10, No. 4, 354-359, (1965).
2. VIKTOROV, I.A., *Rayleigh and Lamb Waves: Physical Theory and Applications*, (Plenum, New York, 1967).
3. DITRI, J.J., ROSE, J.L., "Excitation of guided waves in generally anisotropic layers using finite sources," ASME *J. Appl. Mech.*, Vol. 61, No. 2, 330-338, (1994).
4. DITRI, J.J., RAJANA, K.M. "Analysis of the wedge method of generating guided waves," these proceedings.
5. AULD, B., *Acoustic Fields and Waves in Solids, Vol II*, 2nd Ed., (Kreiger, Malabar FL, 1990),.